Published in final edited form as:
*Cell Motil Cytoskeleton*. 2009 June ; 66(6): 303–316. doi:10.1002/cm.20361.

# N-WASP and cortactin are involved in invadopodium-dependent chemotaxis to EGF in breast tumor cells

**Vera DesMarais**[1], **Hideki Yamaguchi**[2], **Matthew Oser**[1], **Lilian Soon**[4], **Ghassan Mouneimne**[5], **Corina Sarmiento**[1], **Robert Eddy**[1], and **John Condeelis**[1,3]

[1]Department of Anatomy and Structural Biology Albert Einstein College of Medicine 1300 Morris Park Avenue, F628 Bronx, NY, 10461, USA

[2]Laboratory of Genome and Biosignal Tokyo University of Pharmacy and Life Science 1432-1 Horinouchi, Hachioji-city Tokyo 192-0392, Japan

[3]Gruss-Lipper Biophotonics Center Albert Einstein College of Medicine 1300 Morris Park Avenue Bronx, NY, 10461, USA

[4]Australian Centre for Microscopy and Microanalysis Electron Microscope Unit, Madsen Building, F09 The University of Sydney NSW, 2006, AUSTRALIA

[5]Department of Cell Biology Harvard Medical School 240 Longwood Ave, Building C1 Boston, MA 02115, USA

## Abstract

Metastatic mammary carcinoma cells, which have previously been observed to form mature, matrix degrading invadopodia on a thick ECM matrix, are able to form invadopodia with similar characteristics on glass without previously applied matrix. They form in response to EGF, and contain the usual invadopodium core proteins N-WASP, Arp2/3, cortactin, cofilin, and F-actin. The study of invadopodia on glass allows for higher resolution analysis including the use of total internal reflection microscopy and analysis of their relationship to other cell motility events, in particular, lamellipodium extension and chemotaxis toward an EGF gradient. Invadopodium formation on glass requires N-WASP and cortactin but not microtubules. In a gradient of EGF more invadopodia form on the side of the cells facing the source of EGF. In addition, depletion of N-WASP or cortactin, which blocks invadopodium fromation, inhibits chemotaxis of cells towards EGF. This appears to be a localized defect in chemotaxis since depletion of N-WASP or cortactin via siRNA had no effect on lamellipodium protrusion or barbed end generation at the lamellipodium's leading edge. Since chemotaxis to EGF by breast tumor cells is involved in metastasis, inhibiting N-WASP activity in breast tumor cells might prevent metastasis of tumor cells while not affecting chemotaxis-dependent innate immunity which depends on WASp function in macrophages.

## Introduction

In the cell, there are several different compartments that form at the cell periphery that are protrusive and contain actively polymerizing actin. The largest one is the lamellipodium, which is a broad, flat area at the cell periphery that contains branched actin filaments that push the membrane forward to help translocate the cell during the motility cycle (see for example recent review by Le Clainche C [2008]). Another actin-containing structure at the cell periphery is the filopod, which is a long, thin projection that contains bundled actin

Corresponding author: Vera DesMarais (vdesmara@aecom.yu.edu,) Tel.: (718) 430-3547 Fax: (718) 430-8996.

filaments as well as many different actin-binding proteins (see for example recent review by Mattila and Lappalainen [2008]). In addition, on the ventral surface, some specialized cells such as cells of the hematopoetic lineage (e.g. macrophages) form podosomes, while metastatic cancer cells form related structures, the invadopodia [reviewed by Buccione et al., 2004; Calle et al., 2006; Linder, 2007; Linder and Aepfelbacher, 2003; Linder and Kopp, 2005].

Podosomes, as seen in macrophages and other cells of the hematopoetic cell lineage, are non-protrusive dot-like matrix contacts at the ventral cell surface with associated matrix degradation activity. Podosomes contain a core of F-actin and actin-associated proteins, such as WASp, cortactin, and Arp2/3. The core is surrounded by a ring-like structure containing focal adhesion-type molecules such as talin, vinculin, and paxillin. In macrophages, it has been shown that the formation of podosomes is dependent on the Wiskott-Aldrich syndrome protein (WASp) [Linder et al., 1999]. In addition, it has also been shown that macrophages lacking WASp (and thus also lacking podosomes) show a defect in chemotaxis towards a gradient of CSF-1. Interestingly, this defect is not due to a defect in the level of motility, since translocational motility is present to the same extend in WASp-lacking cells and control cells [Zicha et al., 1998]. Cells form dozens of podosomes and they are recruited to sites of cell protrusion and may aid in the stabilization of the protrusion, thus playing a role in directed cell migration [reviewed by Buccione et al., 2004; Calle et al., 2006; Linder, 2007; Linder and Aepfelbacher, 2003; Linder and Kopp, 2005].

Several studies have aimed to elucidate the mechanism of podosome formation and it was found that microtubules are necessary for podosome formation in monocytes and macrophages, since addition of the microtubule-depolymerization drug nocodazole led to failure of podosome formation in monocytes and failure of podosome re-formation in macrophages [Linder et al., 2000]. In addition, it was found that microtubules are also important for the turnover of podosomes, in particular, the cellular fate of podosomes is influenced by contact with microtubule plus ends [Kopp et al., 2006].

Invadopodia, as seen on the ventral surface of metastatic cancer cells, are actin-rich protrusive structures with associated matrix degradation activity [Chen, 1989]. Invadopodia are believed to be important for tumor cells to penetrate the basement membrane of epithelia and blood vessels. Tumor cells lack WASp, but do express the WASp-family member N-WASP. Invadopodia contain many proteins that modulate actin polymerization, such as N-WASP, cortactin, Arp2/3, and dynamin [reviewed by [Buccione et al., 2004; Linder and Aepfelbacher, 2003], and their formation is dependent on cortactin [Bowden et al., 1999], N-WASP [Mizutani et al., 2002; Yamaguchi et al., 2005] and Arp2/3 [Yamaguchi et al., 2005]. Also, cofilin appears to be involved in invadopodium formation, since depletion of cofilin causes invadopodia to be shorter-lived and less invasive [Yamaguchi et al., 2005]. In our model system (metastatic carcinoma MTLn3 cells), formation of invadopodia is EGF dependent, and Cdc42, WIP and Nck1, which are all upstream regulators of N-WASP, are necessary for the formation of invadopodia [Yamaguchi et al., 2005].

The formation of invadopodia can be subdivided into several stages. For MDA-MB-231 cells, the formation has been subdivided into four stages [Artym et al., 2006]. The first stage, invadopodia initiation, is characterized by the initial accumulation of cortactin and actin. The same is true for the second stage, the preinvadopodia stage. In the third stage, the mature invadopodia stage, MT1-MMP is accumulated and matrix degradation is observed. The fourth stage, the late invadopodia stage, is characterized by MT1-MMP presence and matrix degradation but a loss of cortactin and actin staining.

The aim of this study is to investigate whether, in breast tumor cells that are chemotactic to EGF, N-WASP plays a function in chemotaxis similar to WASp in macrophages. Breast tumor cells are non-hematopoetic cells that do not express the WASp protein or form podosomes, but do express N-WASP and form invadopodia. If macrophage chemotaxis depends on WASp while tumor cell chemotaxis depends on N-WASP, this difference in protein type may open up the possibility of specifically targeting chemotaxis in tumor cells while not affecting chemotaxis of blood and immune cells such as macrophages. Since chemotaxis to EGF by breast tumor cells is involved in metastasis [Condeelis and Pollard 2006], inhibiting N-WASP activity in breast tumor cells might prevent metastasis of tumor cells while not affecting the patients' immune system.

Most previous studies have investigated invadopodium formation and function in the context of cells on a thick ECM-matrix and matrix degradation activity. In this study we focus on the initiation of invadopodium formation on glass. This would be equivalent to stages I and II of the invadopodium-formation stages mentioned above. This more standard tissue culture environment allows for higher resolution analysis including total internal reflection microscopy (TIRF) and allows us to relate formation of invadopodia to other cell-motility functions, in particular lamellipodium extension and chemotaxis toward an EGF gradient.

## Experimental Procedures

### Cell culture and EGF stimulation

MTLn3 rat adenocarcinoma cells were cultured as described previously [Bailly et al. 1998b; Segall et al. 1996]. Cells were plated at low densities for at least 24 hours in complete medium. Before addition of EGF, cells were starved in Leibovitz's L15 medium (Gibco) with 0.35% BSA for 3 hours. To stimulate cells, murine epidermal growth factor (EGF) was added at a final concentration of 5 nM (Life Technologies) in starvation medium for the indicated times.

### Cell lines

The stable cell line MTLn3 beta-actin-GFP used in this work has been previously described [Lorenz et al. 2004a]. The dominant negative N-WASP construct has also been described previously [Banzai et al. 2000].

### Immunofluorescence

Cells were plated on dishes with glass bottoms (MatTek Corporation) as previously described [Bailly et al. 1998a]. Cells were fixed with 3.7% formaldehyde, 0.1% glutaraldehyde, 0.15 mg/ml saponin in PBS, followed by treatment with 2 mg/ml NaBH4 in PBS [Eddy, Pierini et al. 2000]. After several washes with PBS, cells were incubated with 1%BSA, 1%FCS in PBS. Cells were incubated with primary antibodies, followed by washes with PBS and secondary antibodies. Primary antibodies used included: polyclonal rabbit anti-N-WASP [Miki et al. 1996], monoclonal mouse anti-cortactin (Upstate), anti-Arp2 (Santa Cruz), anti-cofilin AE774 (a chicken IgY antibody raised against purified recombinant full-length rat cofilin which recognizes both the dephosphorylated and phosphorylated forms of cofilin, purified using T-gel Absorbent (Pierce) and further purified by affinity chromatography against the peptide or protein immunogen), and anti-biotin (Jackson ImmunoResearch Laboratories). Secondary antibodies included: anti-rabbit, anti-mouse, and anti-chick conjugated with appropriate Alexa fluorophores (Molecular Probes). Phalloidin (Calbiochem) was used to stain for F-actin.

### Nocodazole and taxol treatment

For microtubule inhibition experiments, MTLn3 cells plated on glass coverslip dishes (MatTek) overnight were starved for 2 hrs, then treated for 1 hr with 10 μM nocodazole or 5 μM taxol (Sigma-Aldrich). Cells were stimulated with 5 nM EGF for 1 and 3 min in the presence or absence of nocodozole or taxol, fixed and prepared for immunofluorescence as previously described. Invadopodia were indentified using a polyclonal antibody against N-WASP to indentify invadopodia. Microtubule organization was assessed using a monoclonal antibody against α-tubulin (DM1A) (Calbiochem).

### Microscopy

Objective illuminated TIRF was performed on an Olympus IX71 microscope (Olympus America, Center Valley, PA) with 60X N.A. 1.45 optics. Lasers for fluorescence excitation were an Ar 488nm (Melles Griot, Carlsbad, CA) for GFP and FITC and a HeNe 543nm (Melles Griot) for rhodamine and Cy3. A single 460LP dichroic was used and emission fluorescence was detected via narrow pass filters mounted in front of a CoolSnap HQ cooled CCD camera (Photometrics, Tucson, AZ) operated by IPLab software (BD Biosciences, Rockville, MD).

Images for Figure 1A were collected with a Leica TCS SP2 AOBS confocal microscope (Mannheim, Germany) with an Ar laser at 488nm for exciting green and a diode 561nm laser for exciting red. The objective was a 60X N.A. 1.4, line-by-line sequential scanning was used to eliminate crosstalk between channels and 0.2um tetraspeck beads (Molecular Probes Invitrogen, Carlsbad, CA) were used to assure X,Y and Z axis registration.

### siRNA

Depletion of cellular cofilin [Ghosh et al. 2004; Mouneimne et al. 2004], N-WASP [Kempiak et al. 2005; Yamaguchi et al. 2005], Cdc42 [Yamaguchi et al. 2005] and cortactin [Kempiak et al. 2005] was achieved via siRNA treatment as described previously for MTLn3 cells. For this manuscript, expression of dominant negative N-WASP was used to replicate the phenotype of inhibition of chemotaxis.

### Pipette Chemotaxis assay

The live pipette experiments were conducted as previously described [Mouneimne 2006; Mouneimne et al. 2004]. In summary, cells were starved as described above, followed by stimulation with a micropipette (Eppendorf Femtotip II) containing 50 nM EGF. The pipette was placed within 1–2 cell diameters of each experimental cell for 90 seconds, membrane protrusion was monitored via time-lapse microscopy every 10 seconds for a total of 10 minutes after stimulation. An Eppendorf Femtojet pump was used to set the pressure of chemoattractant flow at 15 hPa. The chemotactic index, $\cos\theta$, was measured to assess whether cells were able to protrude towards the EGF gradient, where the angle $\theta$ is the angle between two reference lines; the first line is drawn between the centroid of the cell in the first frame of time-lapsing and the pipette tip location, and the second line is drawn from the centroid of the cell in the first and the last frame of the time-lapse (Figure 5A). Thus the angle $\theta$ indicates how well the cell protrudes in the direction of the pipette. A small angle $\theta$ and a high chemotactic index, with a $\cos\theta$ closer to one, occurs for cells that protrude directly towards the pipette.

For the fixed pipette assay in Figure 3, cells were stimulated with an EGF-containing micropipette for 90 seconds as above, but they were fixed and stained after a total of 3 minutes. With the aid of gridded coverslips we then imaged previously pipette-stimulated cells as well as unstimulated control cells by TIRF microscopy

Experiments using the Soon chamber have been previously described (Soon et al. 2005). This chamber consists of a micopipette filled with EGF and a glass-bottom chamber containing a coverslip on which MTLn3 cells were grown. The coverslip acts as a dam against which the micropipette is placed. This dam creates a steep gradient of chemoattractant that retains stability over the course of the experiment.

### Quantification of dots (invadopodia) using image J

Images of cells stained for N-WASP or cortactin to identify invadopodia were imported into image J. A threshold was applied so that large dots were included in the threshold, but not very small dots (1–2 pixels). Then particle size and frequency were analyzed using the "Analyze Particle" command. This vastly underestimated the number of very small dots (1–2 pixels), however, it was not possible to set the threshold in a way to include all of the very small particles and maintain separation of large particles. Thus, a cut-off of 10 pixels as the minimal particle size was used. At the magnification used, if the structures were perfectly circular, a 10-pixel area would be equivalent to a circle with a diameter of 1.7 um. However, many were not circular and many were much larger that 10 pixels.

## Results

### EGF stimulation induces the formation of invadopodia in carcinoma cells plated on glass, very close to the ventral membrane surface

We stained cells plated on glass for N-WASP and cortactin, proteins previously shown to be present in invadopodia of these metastatic tumor cells plated on a thick collagen matrix [Yamaguchi et al. 2005]. Images of the cells in the z-dimension were obtained using a confocal microscope before and after EGF stimulation (Figure 1A) and revealed that N-WASP and cortactin are both present in large dots very close to the ventral surface of the cell. To determine how close, we used TIRF microscopy, and found that TIRF tuned for high resolution imaging shows these structures at the ventral surface of cells within 150 nm of the glass. Hence, TIRF is ideal for characterizing the initial formation of this N-WASP and cortactin containing ventral compartment (Figure 1). All further images were thus taken by TIRF microscopy to characterize these structures at the ventral membrane-surface of MTLn3 cells. The thick matrix used previously [Yamaguchi et al. 2005] is too thick to be within the 150 nm TIRF field, thus it is not possible to use this matrix with TIRF to observe initiation.

In order to examine the cellular localization pattern of N-WASP by TIRF-microscopy we fixed and stained MTLn3 cells that were either unstimulated or stimulated with EGF for 1 or 3 minutes (Figure 1B–D). We found N-WASP to be localized in large, cytoplasmic, cortactin-rich dots at the ventral surface of the cells, and with EGF stimulation there was an increase in these structures.

To determine by TIRF microscopy if the cortactin dots mature into invadopodia with ECM degradation activity, we plated cells on a thin (50 nm thick) matrix of FITC-gelatin [Bowden et al. 2001]. This thin matrix assay has been routinely used to show degradation competence of invadopodia in the past by epifluorescence [Artym et al. 2006; Ayala et al. 2008; Bowden et al. 2001; Mueller et al. 1999]. Degradation areas are black against the background of labeled FITC-gelatin (Figure 1E). Arrows indicate co-localization of cortactin dots with degradation activity indicating their maturation into invadopodia.

### Invadopodia on glass contain Arp2/3, cofilin, and actin filaments

Evidence that the cortactin dots on the ventral surface are functional invadopodia predicted that they should have the usual protein complement present in invadopodia. Further co-

staining experiments showed that cofilin and Arp2/3 complex are present in these TIRF-visualized invadopodia along with cortactin (Figure 2 A,B). We also examined the association of different actin polymerization probes with invadopodia in cells stimulated with EGF for 1 minute. MTLn3 cells transfected with beta-actin-GFP [Lorenz et al. 2004a] and co-stained for N-WASP (Figure 2C) confirmed the presence of actin (see arrows). Phalloidin and cortactin co-staining (Figure S1) confirmed the presence of F-actin (see arrows). To investigate whether actin is actively polymerizing in invadopodia, barbed end assays utilizing biotin-actin incorporation into permeabilized cells [Chan et al. 2000] with cortactin co-staining were conducted and showed the presence of newly polymerizing actin in these structures (see arrows, Figure S1).

In conclusion, the structures observed in TIRF contain typical invadopodial markers, including cortactin, N-WASP, Arp2/3 and actin, and therefore are not just aggregates of cortactin. TIRF allows these structures to be viewed as invadopodia in their initiation/preinvadopodia stages, stages I and II, as previously defined [Artym et al. 2006], when EGF-stimulation is conducted for only up to 3 min.

## The cortactin and N-WASP containing dots seen in TIRF are not vesicles

In order to examine whether these large cortactin/N-WASP dots are large vesicles, we conducted several co-localization experiments using endocytotic markers (Figure S2). For example, clathrin and transferrin-488 localized in small dots that were distinct from the large dots seen by N-WASP or cortactin staining. Also, the endocytic compartments positive for EGF-receptor-GFP were distinct from the large dots containing N-WASP (Figure S2D). Previously, N-WASP and the EGF-receptor have both been localized to small, clathrin-positive endocytic vesicles in cells [Benesch et al. 2005]. In the left inset in Figure S2D, we show some EGF-receptor (green)-positive vesicles with N-WASP (red) staining on the side of the vesicle, similar to previously published clathrin-positive vesicles that show N-WASP-staining associated with them [Benesch et al. 2005]. For comparison, the right inset in Figure S2D shows typical large, N-WASP (red) containing invadopodia. The large dots are not associated with EGF-receptor vesicles and are much larger than the small N-WASP dots that associate with EGF-receptor vesicles, indicating that they are a distinct structure. To investigate whether the large dots are due to fluid-phase pinocytosis, we stimulated cells with EGF for 3 minutes in the presence of FITC-dextran (MW 10000) (Figure S2E), according to a previously described protocol for stimulating pinocytosis [Araki 1998]. Figure S2E shows bright staining of FITC-dextran containing endosomes. However, staining for N-WASP shows that these vesicles are not the same cellular compartment as the N-WASP containing large dots.

## N-WASP, cortactin and Cdc42 are necessary for EGF induced invadopodium formation on glass

The overall requirement for N-WASP and cortactin on invadopodium formation in MTLn3 cells has been previously established [Yamaguchi et al. 2005]. However, since previous experiments were conducted in serum and on a thick matrix, and our study utilizes EGF stimulation to examine the relationship of invadopodium formation and chemotaxis on glass, we investigated if invadopodium formation on glass depends on N-WASP and cortactin during EGF stimulation. MTLn3 cells were treated with siRNA targeting N-WASP or cortactin, or with control siRNA. Invadopodia were visualized by cortactin or N-WASP immunofluorescent staining (Figure 3A). After siRNA treatment targeting N-WASP or cortactin, few cells formed invadopodia after EGF stimulation. After siRNA treatment targeting cofilin, invadopodium assembly was delayed.

Quantification of the data is shown in Figure 3B. Cells were scored as percentage of cells containing invadopodia. Control siRNA treated cells showed an increase in percentage of cells with these structures after EGF stimulation, from around 40% before to around 70% after 3 minutes of EGF stimulation. Both N-WASP and cortactin siRNA-treated cells showed a two-fold decrease of percent of cells with the invadopodia before EGF stimulation compared to control cells. EGF-stimulation did not result in any increase in cells with invadopodia, and the percentage of cells with invadopodia remained under 20%, indicating that both N-WASP and cortactin are required for EGF-induced formation of invadopodia on glass. Depletion of Cdc42 had the same effect as depletion of N-WASP (Figure 3), thus it is likely that N-WASP in the structures is activated via a Cdc42 dependent pathway.

Cells treated with cofilin siRNA showed a smaller decrease in percent of cells with invadopodia before EGF stimulation. After 1 min of EGF, around 40% of cofilin depleted cells had invadopodia, compared to around 70% in control cells. After 3 min of EGF, cofilin depleted cells had similar percentages of invadopodia as control cells. Thus, while cofilin does not appear to be required for invadopodium-formation, lack of cofilin significantly slows invadopodium formation.

## Disruption or stabilization of microtubules has no effect on invadopodium formation

Previously, it has been shown that an intact microtubule system is necessary for the formation of podosomes in monocytes and macrophages [Linder et al. 2000]. In particular, it was shown that treatment of monocytes with the microtubule depolymerization drug nocodazole prevented formation of podosomes during adhesion. Also, after podosomes in macrophages were disassembled by either disruption of the F-actin rich core using cytochalasin D or by blocking tyrosine phosphorylation using tyrosine kinase inhibitor PP2, macrophages were unable to reform podosomes in the presence of nocodazole [Linder et al. 2000]. In order to determine whether the formation of invadopodia in our N-WASP dependent cell system also requires microtubules, we starved cells to reduce levels of invadopodia to basal levels and then treated cells with the microtubule depolymerization drug nocodazole for one hour, followed by EGF stimulation in the presence of nocodalzole (Figure 4A). Unlike podosomes in macrophages or monocytes, nocodazole treated MTLn3 cells formed invadopodia after EGF stimulation to the same levels as untreated cells. Staining of MTLn3 cells with anti-tubulin confirmed disruption of microtubules (data not shown). We also treated MTLn3 cells with the microtubule stabilizing drug taxol, and again, cells were able to form invadopodia to the same levels as control cells after EGF stimulation (Figure 4B), indicating that the formation of invadopodia is independent of dynamic microtubules.

## Invadopodia form preferentially towards an EGF gradient

We examined the formation of invadopodia in an EGF-gradient using a micropipette (Figure 5A). In order to quantify invadopodium-formation towards the pipette, we quantified the structures in the front (facing the pipette) and back (facing away from the pipette) of the cells. In this assay, invadopodia are defined as having a size (area) of at least 10 pixels. This size was chosen for two reasons. One, dots smaller then 10 pixels did not consistently label for both invadopodium markers cortactin and N-WASP. Two, invadopodia that degrade matrix are in this size range. This means that, if invadopodia were perfectly circular, they would have a minimum diameter of 1.7 um. For comparison, invadopodia were also quantified in unstimulated control cells as well as cells uniformly simulated with EGF for 3 minutes (Figure 5B). There was a two-fold (200%) increase in invadopodium number in the front versus the back of pipette-stimulated cells compared to control cells (Figure 5C). Calibration of the EGF gradient between the front and the back of the cell in this assay demonstrates that the gradient is 27% and that the EGF receptor activation follows this 27%

gradient [Mouneimne et al. 2006]. These measurements indicate that there is no amplification of the gradient asymmetry at the level of the EGF receptor. Considering that 40% of cells already contain invadopodia in random locations in the cell before EGF stimulation, the 200% asymmetry of invadopodia in a 27% gradient suggests amplification of the signal generating the asymmetric distribution of invadopodia relative to the EGF gradient. Thus the formation of invadopodia toward the direction of the EGF gradient cannot result from the asymmetry of activation of the EGF-receptors alone, indicating that there is amplification of the EGF signaling to invadopodium formation. This suggests that these asymmetrically distributed invadopodia may be involved in chemotactic sensing. .

### Cells depleted of N-WASP or cortactin (and thus invadopodia) show a defect in directional protrusion toward EGF

We tested if invadopodia are involved in chemotactic sensing. First, we examined whether depletion of N-WASP had an effect on the ability of cells to protrude towards a micropipette containing EGF. As a measure of the ability of cells to protrude toward EGF, we measured the chemotactic index cosθ for control MTLn3 cells, as well as cells treated with N-WASP siRNA, using time-lapse microscopy of cells stimulated with an EGF gradient using a pipette as described previously [Mouneimne et al. 2006] (see Figure 6A). A small angle θ and a high chemotactic index, with a cosθ close to one, occur for cells that protrude toward the pipette. A random angle θ and a low average chemotactic index, with an average cosθ closer to zero, occur for cells that do not preferentially protrude towards the pipette but instead protrude in random directions. As shown in Figure 6B, cells treated with control siRNA showed a much higher chemotactic index than cells treated with N-WASP siRNA, which protruded at random angles, resulting in a low chemotactic index. The same result was obtained using dominant negative N-WASP (Figure S3A). In another approach, we used a Soon chamber, which also measures chemotactic locomotion toward a gradient of EGF [Soon et al. 2005]. Again, N-WASP depleted cells had a very low chemotactic index compared to control (Figure S3B). In addition, cortactin siRNA treated cells displayed the same type of chemotactic defect as N-WASP siRNA treated cells, giving a very low average chemotactic index cosθ (Figure 6C).

Figure 6D and E show the angle distributions that correspond to the cosθ analysis. The majority of control cells have relatively small protrusion angles (<50), overall protruding towards the pipette. Cells treated with N-WASP or cortactin siRNA have a random distribution of angles, with cells distributing fairly evenly over the whole range of angles (0–180).

To demonstrate that siRNA treated cells were still protruding, we also analyzed the cells for front/back protrusion (Figure 6F,G). Control cells showed preferential protrusion at the front (towards the pipette) versus the back (away from the pipette). Cells treated with either N-WASP or cortactin siRNA showed essentially equal front and back protrusion, indicating that they protrude randomly, that protrusion is not inhibited and that they do not sense the EGF gradient. This result is consistent with the observation that N-WASP and cortactin are not required for lamellipodium protrusion (Figure S4 and Sarmiento et al. [2008]).

## Discussion

In this study we have shown that in carcinoma cells, after EGF stimulation, invadopodia that contain N-WASP, cortactin, actin, cofilin and Arp2/3 form within 3 minutes within 150 nm of the glass substrate on the ventral cell surface. Since we studied invadopodial structures that formed within 3 min of EGF-stimulation in cells that were plated on glass, these structures should be viewed as invadopodia in their initiation stages, ie. stages I and II, as previously described [Artym et al. 2006]. When cells are plated on a degradable matrix,

degradation (stage III) commences with a ~6 min delay compared to the beginning of cortactin accumulation in MDA-MB-231 cells [Artym et al. 2006]. For the MTLn3 cells used in our study, the delay between initial cortactin accumulation and degradation is also delayed by many minutes (personal communication, Matthew Oser). By using glass instead of a thick collagen matrix we have increased the substrate rigidity that the cells encounter. A recent study [Alexander et al. 2008] has shown that increasing matrix rigidity promotes the formation of active invadopodia, thus it is not surprising that the early stages of invadopodia readily occur on a rigid glass surface.

We found that depletion of N-WASP, cortactin or Cdc42 eliminates EGF induced invadopodium formation, while depletion of cofilin only slows formation. This confirms that the invadopodia that form on glass have the same molecular characteristics as those previously described for invadopodia on thick matrix [Yamaguchi et al. 2005]. In addition, depletion of either N-WASP or cortactin did not affect the initiation of lamellipodium protrusion or F-actin accumulation at the leading edge of the lamellipodium, indicating that the invadopodium is an actin filament polymerization compartment that is distinct from the leading edge of the lamellipodium. In addition, unlike the requirement for microtubules in podosome formation [Linder et al. 2000], we found that inhibition of microtubule stability and dynamics did not affect invadopodium formation in breast carcinoma cells. Finally, we found that invadopodia form preferentially on the side of the cell facing an EGF gradient source and that the asymmetric formation of these early stage invadopodia is correlated with the directional protrusion of the cell surface toward the EGF source.

## N-WASP and cortactin are necessary for invadopodium formation and function

Our results are consistent with previous studies where N-WASP has been shown to be active in invadopodia [Lorenz et al. 2004] and required for invadopodium formation [Yamaguchi et al. 2005]. However, here we have shown for the first time that N-WASP is required for the **initiation** of invadopodia, while in the same cells, is neither involved in actin polymerization dynamics at the leading edge nor lamellipodium protrusion. The lack of N-WASP involvement in lamellipodium protrusion is supported by previous studies using N-WASP knock-out and siRNA knock-down cells, which display normal morphologies and are able to spread and extend large lamellipodia after stimulation with growth factors [Lommel et al. 2001; Sarmiento et al. 2008; Snapper et al. 2001; Yu et al. 2006]. Also, N-WASP depleted human fibrosarcoma cells undergoing random motility in serum show no defect in lamellipodium persistence, protrusion velocity, or protrusion distance [Bryce et al. 2005].

We have shown previously that N-WASP activity is present in lamellipodia as well as in the invadopodia of tumor cells [Lorenz et al. 2004b]. Since invadopodium formation often initiates at the cell periphery in the lamellipodia of tumor cells followed by migration of invadopodia centripetally [Yamaguchi et al. 2005], N-WASP activity may function in the lamellipodium in the initiation of invadopodia in this peripheral location but not contribute to lamellipodial function. An example of the formation of invadopodia near the cell periphery in our tissue culture system is shown in Figure S5.

Cortactin is a major constituent of the invadopodium and in our study was the most robust and consistent marker for the early appearance of the invadopodium. Cortactin is essential for the formation of invadopodia since siRNA depletion of cortactin caused inhibition of the earliest stages of invadopodia. Previously, cortactin has been implicated in the stabilization of N-WASP and Arp2/3 complex induced dendritic nucleation branch points [Uruno et al. 2003; Weaver et al. 2001], a role it may also play in invadopodium formation.

The role of cortactin in lamellipodium protrusion is more complex than that of N-WASP. While cortactin depletion does not appear to inhibit initial lamellipodium protrusion, it does appear to play a role in lamellipodium stabilization and maintenance as well as invadopodium formation. For example, in previous studies examining random motility in serum, cortactin-depleted MTLn3 cells appeared to have less stable lamellipodia [Kempiak et al. 2005]. Also, cortactin depleted cells undergoing random motility showed a decrease in lamellipodium persistence [Bryce et al., 2005]. However, just as found in our study, cortactin does not appear necessary in the initiation of lamellipodium protrusion since protrusion velocity, retraction velocity and protrusion distance where unchanged in cortactin depleted cells [Bryce et al., 2005]. In spite of the dual role played by cortactin in both lamellipodium stabilization and invadopodium formation, we conclude that in our case, it is the lack of cortactin function in invadopodium formation, and not in lamellipodium protrusion, which is the important factor in diminished directional protrusion. Our chemotaxis assay is short in duration (<10 min), focusing on the initial sensing and directional protrusion of cells and our data show that within this time-frame cortactin depleted cells form stable lamellipodia and do not show signs of retraction or instability.

## Cofilin and the regulation of invadopodium maturation

The observation that depletion of cofilin slows formation of invadopodia is consistent with previous work showing that the depletion of cofilin in MTLn3 cells decreases the rate of protrusion of lamellipodia (Sidani et al. 2007). However, the depletion of cofilin was found to decrease the stability of invadopodia [Yamaguchi et al. 2005] while increasing the stability of lamellipodia [Sidani et al. 2007], indicating that cofilin has opposite effects on the stability of invadopodia and lamellipodia in cancer cells. These results further support the idea that the invadopodium is an actin filament polymerization compartment that is distinct from the leading edge of the lamellipodium.

At the leading edge of the lamellipodium, cofilin functions synergistically with the Arp2/3 complex to initiate actin polymerization to support Arp2/3 complex-mediated dendritic nucleation and protrusion during tumor cell migration and chemotaxis [Sidani et al. 2007; van Rheenen et al. 2007]. However, the function of cofilin in invadopodia is not well understood. The opposite effects of cofilin depletion on invadopodium and lamellipodium stability but similar effects on initiation of formation of both suggests that cofilin functions similarly in the initiation of actin polymerization in both locations but does not function in filament depolymerization in invadopodia. More work is required to define these similarities and differences at the molecular level.

## Invadopodia and chemotaxis

Invadopodia formed preferably on the side of the cell facing an EGF gradient, suggesting their involvement in directional polarization of cells toward the gradient. The asymmetric formation of invadopodia on the side of the cell facing the EGF gradient does not correlate in magnitude with the asymmetric activation of EGF-receptors, because the 200% asymmetry of invadopodia in a 27% gradient of EGF-receptor activation requires asymmetric amplification of the EGF signal. In a previous paper we have investigated the amplification of the EGF signal through PLC to cofilin-dependent actin barbed-end formation [Mouneimne et al. 2006] and found that while both PLC and cofilin activities are found on the side of the cell facing the EGF gradient, phospho-PLC activity showed little amplification of the EGF gradient while cofilin dependent barbed end production shows a 8–10 fold amplification. This indicates that the gradient amplification does not occur at the level of EGF receptor signaling to PLC, but occurs downstream at the level of cofilin dependent formation of actin barbed-ends. This lack of signal amplification at the level of EGF-receptor, and the fact that we found an 8-fold amplification of the 27% EGF gradient

when formation of invadopodia was measured in our study indicates that the cell may use invadopodia as a signal sensing and amplification mechanism.

Inhibition of formation of invadopodia by depletion of either N-WASP or cortactin coincided with a loss of directional protrusion toward the EGF gradient but not global protrusion. This loss of chemotatic sensing of a micropipette containing EGF cannot be explained by a simple loss of lamellipodium protrusion, since cells depleted of either N-WASP or cortactin with siRNA showed normal initiation of lamellipodium protrusion in response to EGF (Figure S4). Also, like control cells, N-WASP and cortactin siRNA treated cells still showed lamellipodium protrusion when stimulated with EGF delivered from a micropipette (Figure 6 F, G). The difference between control and either N-WASP or cortactin depleted cells was that control cells showed protrusions in the front of the cell facing the pipette and not the back, while depleted cells showed protrusions at both the front and the back. The front-protrusion of depleted cells was diminished compared to control, but the sum of front and back protrusion of depleted cells was approximately equal to the front protrusion observed in control cells (Figure 6). Thus the phenotype resulting from depletion of either N-WASP or cortactin appears to be a true defect in chemotaxis, where cells are still able to extend lamellipodia, but do not preferentially extend in the direction of the EGF gradient. In addition, these results indicate that the invadopodium, while not being required for lamellipodium protrusion, may be involved in setting the direction of protrusion when it occurs.

Our results share parallels with results obtained for WASp and podosomes in macrophages. In macrophages, the formation of podosomes is dependent on WASp [Linder et al. 1999] and cells depleted of WASp do not chemotax towards CSF1 [Zicha et al. 1998]. In addition, while WASp-deficient macrophages have a defect in chemotaxis, they still maintain normal cell speed, thus non-directional cell motility is not affected [Zicha et al. 1998]. However, a link between WASp-dependent chemotaxis and podosome formation has not been established, while our results link formation of invadopodia with the direction of the chemotactic gradient and chemotaxis. Our results also show, for the first time, that chemotaxis in tumor cells, which do not express WASp, is dependent on N-WASP.

The reason that it is important to investigate and highlight the differences in macrophage and tumor cell chemotaxis, the former depending on WASp and the latter on N-WASP, is that this difference in mechanism may yield an opportunity to target the chemotaxis and thus metastasis of tumor cells while not affecting the chemotaxis of immune cells such as macrophages, thus leaving the patients' immune system intact.

The question that remains at this point is, how do invadopodia contribute to chemotactic sensing of the EGF gradient. One possibility is that the formation of invadopodia links the actin cytoskeleton to other mechanisms of establishing cell polarity, such as microtubule orientation. It has been found in many cell types that the microtubule-organizing center (MTOC) is repositioned between the leading edge and the nucleus in directional cell migration (see for example Gomes et al. 2005)). Also, microtubule involvement in podosome function is suggested by recent data implicating microtubules in podosome dynamics [Kopp et al. 2006]. However, our study indicates that unlike podosomes, invadopodium formation is independent of the microtubule system, since disruption of microtubules using nocodazole or stabilization of microtubules using taxol had no effect on invadopodium formation. Thus it is unlikely that microtubules are the link between cell polarization and invadopodium, formation in breast tumor cells.

Other possibilities include affects on adhesion stability in the areas of the cell facing the chemotactic gradient. Recently it was found that the formation of invadopodia is dependent

on the contractile apparatus of the cell, specifically muscle myosin II, myosin light chain kinase, and Rho kinase [Alexander et al. 2008[. Interestingly, myosin II does not localize in invadopodia, but is thought to act at a distance via the mechanosensing proteins p130Cas and focal adhesion kinase (FAK), which do localize to invadopodia [Alexander et al. 2008]. Invadopodia could affect chemotactic sensing by influencing membrane trafficking, which has been implicated in cell polarity. In addition it is possible that invadopodia allow detection of haptotactic signals, thereby inducing chemotactic sensing. The exact relationship of invadopodium formation and chemotaxis will require additional work to evaluate these distinct possibilities.

## Supplementary Material

Refer to Web version on PubMed Central for supplementary material.

## Acknowledgments

We would like to thank Dr. Tadaomi Takenawa for the N-WASP antibody and constructs. We would like to thank the Analytical Imaging Facility and especially Michael Cammer and David Entenberg at the A. Einstein College of Medicine for help with microscopy. Funding was provided via NIH Grant# GM38511 to John Condeelis.

## References

Alexander NR, Branch KM, Parekh A, Clark ES, Iwueke IC, Guelcher SA, Weaver AM. Extracellular matrix rigidity promotes invadopodia activity. Curr Biol. 2008; 18(17):1295–9. [PubMed: 18718759]

Araki NaS, JA. Cell Biology: A Laboratory Handbook. Academic Press; 1998.

Artym VV, Zhang Y, Seillier-Moiseiwitsch F, Yamada KM, Mueller SC. Dynamic interactions of cortactin and membrane type 1 matrix metalloproteinase at invadopodia: defining the stages of invadopodia formation and function. Cancer Res. 2006; 66(6):3034–43. [PubMed: 16540652]

Ayala I, Baldassarre M, Giacchetti G, Caldieri G, Tete S, Luini A, Buccione R. Multiple regulatory inputs converge on cortactin to control invadopodia biogenesis and extracellular matrix degradation. J Cell Sci. 2008; 121(Pt 3):369–78. [PubMed: 18198194]

Bailly M, Condeelis JS, Segall JE. Chemoattractant-induced lamellipod extension. Microsc Res Tech. 1998a; 43(5):433–43. [PubMed: 9858340]

Bailly M, Yan L, Whitesides GM, Condeelis JS, Segall JE. Regulation of protrusion shape and adhesion to the substratum during chemotactic responses of mammalian carcinoma cells. Exp Cell Res. 1998b; 241(2):285–99. [PubMed: 9637770]

Banzai Y, Miki H, Yamaguchi H, Takenawa T. Essential role of neural Wiskott-Aldrich syndrome protein in neurite extension in PC12 cells and rat hippocampal primary culture cells. J Biol Chem. 2000; 275(16):11987–92. [PubMed: 10766829]

Benesch S, Polo S, Lai FP, Anderson KI, Stradal TE, Wehland J, Rottner K. N-WASP deficiency impairs EGF internalization and actin assembly at clathrin-coated pits. J Cell Sci. 2005; 118(Pt 14): 3103–15. [PubMed: 15985465]

Bowden ET, Barth M, Thomas D, Glazer RI, Mueller SC. An invasion-related complex of cortactin, paxillin and PKCmu associates with invadopodia at sites of extracellular matrix degradation. Oncogene. 1999; 18(31):4440–9. [PubMed: 10442635]

Bowden ET, Coopman PJ, Mueller SC. Invadopodia: unique methods for measurement of extracellular matrix degradation in vitro. Methods Cell Biol. 2001; 63:613–27. [PubMed: 11060862]

Bryce NS, Clark ES, Leysath JL, Currie JD, Webb DJ, Weaver AM. Cortactin promotes cell motility by enhancing lamellipodial persistence. Curr Biol. 2005; 15(14):1276–85. [PubMed: 16051170]

Buccione R, Orth JD, McNiven MA. Foot and mouth: podosomes, invadopodia and circular dorsal ruffles. Nat Rev Mol Cell Biol. 2004; 5(8):647–57. [PubMed: 15366708]

Calle Y, Burns S, Thrasher AJ, Jones GE. The leukocyte podosome. Eur J Cell Biol. 2006; 85(3-4): 151–7. [PubMed: 16546557]

Chan AY, Bailly M, Zebda N, Segall JE, Condeelis JS. Role of cofilin in epidermal growth factor-stimulated actin polymerization and lamellipod protrusion. J Cell Biol. 2000; 148(3):531–42. [PubMed: 10662778]

Chen WT. Proteolytic activity of specialized surface protrusions formed at rosette contact sites of transformed cells. J Exp Zool. 1989; 251(2):167–85. [PubMed: 2549171]

Condeelis J, Pollard JW. Macrophages: obligate partners for tumor cell migration, invasion, and metastasis. Cell. 2006; 124(2):263–6. [PubMed: 16439202]

Ghosh M, Song X, Mouneimne G, Sidani M, Lawrence DS, Condeelis JS. Cofilin promotes actin polymerization and defines the direction of cell motility. Science. 2004; 304(5671):743–6. [PubMed: 15118165]

Gomes ER, Jani S, Gundersen GG. Nuclear movement regulated by Cdc42, MRCK, myosin, and actin flow establishes MTOC polarization in migrating cells. Cell. 2005; 121(3):451–63. [PubMed: 15882626]

Kempiak SJ, Yamaguchi H, Sarmiento C, Sidani M, Ghosh M, Eddy RJ, Desmarais V, Way M, Condeelis J, Segall JE. A neural Wiskott-Aldrich Syndrome protein-mediated pathway for localized activation of actin polymerization that is regulated by cortactin. J Biol Chem. 2005; 280(7):5836–42. [PubMed: 15579908]

Kopp P, Lammers R, Aepfelbacher M, Woehlke G, Rudel T, Machuy N, Steffen W, Linder S. The kinesin KIF1C and microtubule plus ends regulate podosome dynamics in macrophages. Mol Biol Cell. 2006; 17(6):2811–23. [PubMed: 16554367]

Le Clainche CCM. Regulation of actin assembly associated with protrusion and adhesion in cell migration. Physiol Rev. 2008; 88(2):489–513. [PubMed: 18391171]

Linder S. The matrix corroded: podosomes and invadopodia in extracellular matrix degradation. Trends Cell Biol. 2007; 17(3):107–17. [PubMed: 17275303]

Linder S, Aepfelbacher M. Podosomes: adhesion hot-spots of invasive cells. Trends Cell Biol. 2003; 13(7):376–85. [PubMed: 12837608]

Linder S, Hufner K, Wintergerst U, Aepfelbacher M. Microtubule-dependent formation of podosomal adhesion structures in primary human macrophages. J Cell Sci. 2000; 113(Pt 23):4165–76. [PubMed: 11069762]

Linder S, Kopp P. Podosomes at a glance. J Cell Sci. 2005; 118(Pt 10):2079–82. [PubMed: 15890982]

Linder S, Nelson D, Weiss M, Aepfelbacher M. Wiskott-Aldrich syndrome protein regulates podosomes in primary human macrophages. Proc Natl Acad Sci U S A. 1999; 96(17):9648–53. [PubMed: 10449748]

Lommel S, Benesch S, Rottner K, Franz T, Wehland J, Kuhn R. Actin pedestal formation by enteropathogenic Escherichia coli and intracellular motility of Shigella flexneri are abolished in N-WASP-defective cells. EMBO Rep. 2001; 2(9):850–7. [PubMed: 11559594]

Lorenz M, DesMarais V, Macaluso F, Singer RH, Condeelis J. Measurement of barbed ends, actin polymerization, and motility in live carcinoma cells after growth factor stimulation. Cell Motil Cytoskeleton. 2004a; 57(4):207–17. [PubMed: 14752805]

Lorenz M, Yamaguchi H, Wang Y, Singer RH, Condeelis J. Imaging sites of N-wasp activity in lamellipodia and invadopodia of carcinoma cells. Curr Biol. 2004b; 14(8):697–703. [PubMed: 15084285]

Mattila PK, Lappalainen P. Filopodia: molecular architecture and cellular functions. Nat Rev Mol Cell Biol. 2008; 9(6):446–454. [PubMed: 18464790]

Miki H, Miura K, Takenawa T. N-WASP, a novel actin-depolymerizing protein, regulates the cortical cytoskeletal rearrangement in a PIP2-dependent manner downstream of tyrosine kinases. Embo J. 1996; 15(19):5326–35. [PubMed: 8895577]

Mizutani K, Miki H, He H, Maruta H, Takenawa T. Essential role of neural Wiskott-Aldrich syndrome protein in podosome formation and degradation of extracellular matrix in src-transformed fibroblasts. Cancer Res. 2002; 62(3):669–74. [PubMed: 11830518]

Mouneimne G, DesMarais V, Sidani M, Scemes E, Wang W, Song X, Eddy R, Condeelis J. Spatial and temporal control of cofilin activity is required for directional sensing in carcinoma cells. Curr Biol accepted. 2006

Mouneimne G, Soon L, DesMarais V, Sidani M, Song X, Yip SC, Ghosh M, Eddy R, Backer JM, Condeelis J. Phospholipase C and cofilin are required for carcinoma cell directionality in response to EGF stimulation. J Cell Biol. 2004; 166(5):697–708. [PubMed: 15337778]

Mueller SC, Ghersi G, Akiyama SK, Sang QX, Howard L, Pineiro-Sanchez M, Nakahara H, Yeh Y, Chen WT. A novel protease-docking function of integrin at invadopodia. J Biol Chem. 1999; 274(35):24947–52. [PubMed: 10455171]

Sarmiento C, Wang W, Dovas A, Yamaguchi H, Sidani M, El-Sibai M, Desmarais V, Holman HA, Kitchen S, Backer JM, et al. WASP family members and formin proteins coordinate regulation of cell protrusions in carcinoma cells. J Cell Biol. 2008; 180(6):1245–60. [PubMed: 18362183]

Segall JE, Tyerech S, Boselli L, Masseling S, Helft J, Chan A, Jones J, Condeelis J. EGF stimulates lamellipod extension in metastatic mammary adenocarcinoma cells by an actin-dependent mechanism. Clin Exp Metastasis. 1996; 14(1):61–72. [PubMed: 8521618]

Sidani M, Wessels D, Mouneimne G, Ghosh M, Goswami S, Sarmiento C, Wang W, Kuhl S, El-Sibai M, Backer JM, et al. Cofilin determines the migration behavior and turning frequency of metastatic cancer cells. J Cell Biol. 2007; 179(4):777–91. [PubMed: 18025308]

Snapper SB, Takeshima F, Anton I, Liu CH, Thomas SM, Nguyen D, Dudley D, Fraser H, Purich D, Lopez-Ilasaca M, et al. N-WASP deficiency reveals distinct pathways for cell surface projections and microbial actin-based motility. Nat Cell Biol. 2001; 3(10):897–904. [PubMed: 11584271]

Soon L, Mouneimne G, Segall J, Wyckoff J, Condeelis J. Description and characterization of a chamber for viewing and quantifying cancer cell chemotaxis. Cell Motil Cytoskeleton. 2005; 62(1):27–34. [PubMed: 16025469]

Uruno T, Liu J, Li Y, Smith N, Zhan X. Sequential interaction of actin-related proteins 2 and 3 (Arp2/3) complex with neural Wiscott-Aldrich syndrome protein (N-WASP) and cortactin during branched actin filament network formation. J Biol Chem. 2003; 278(28):26086–93. [PubMed: 12732638]

van Rheenen J, Song X, van Roosmalen W, Cammer M, Chen X, Desmarais V, Yip SC, Backer JM, Eddy RJ, Condeelis JS. EGF-induced PIP2 hydrolysis releases and activates cofilin locally in carcinoma cells. J Cell Biol. 2007; 179(6):1247–59. [PubMed: 18086920]

Weaver AM, Karginov AV, Kinley AW, Weed SA, Li Y, Parsons JT, Cooper JA. Cortactin promotes and stabilizes Arp2/3-induced actin filament network formation. Curr Biol. 2001; 11(5):370–4. [PubMed: 11267876]

Yamaguchi H, Lorenz M, Kempiak S, Sarmiento C, Coniglio S, Symons M, Segall J, Eddy R, Miki H, Takenawa T, et al. Molecular mechanisms of invadopodium formation: the role of the N-WASP-Arp2/3 complex pathway and cofilin. J Cell Biol. 2005; 168(3):441–52. [PubMed: 15684033]

Yu N, Atienza JM, Bernard J, Blanc S, Zhu J, Wang X, Xu X, Abassi YA. Real-time monitoring of morphological changes in living cells by electronic cell sensor arrays: an approach to study G protein-coupled receptors. Anal Chem. 2006; 78(1):35–43. [PubMed: 16383308]

Zicha D, Allen WE, Brickell PM, Kinnon C, Dunn GA, Jones GE, Thrasher AJ. Chemotaxis of macrophages is abolished in the Wiskott-Aldrich syndrome. Br J Haematol. 1998; 101(4):659–65. [PubMed: 9674738]

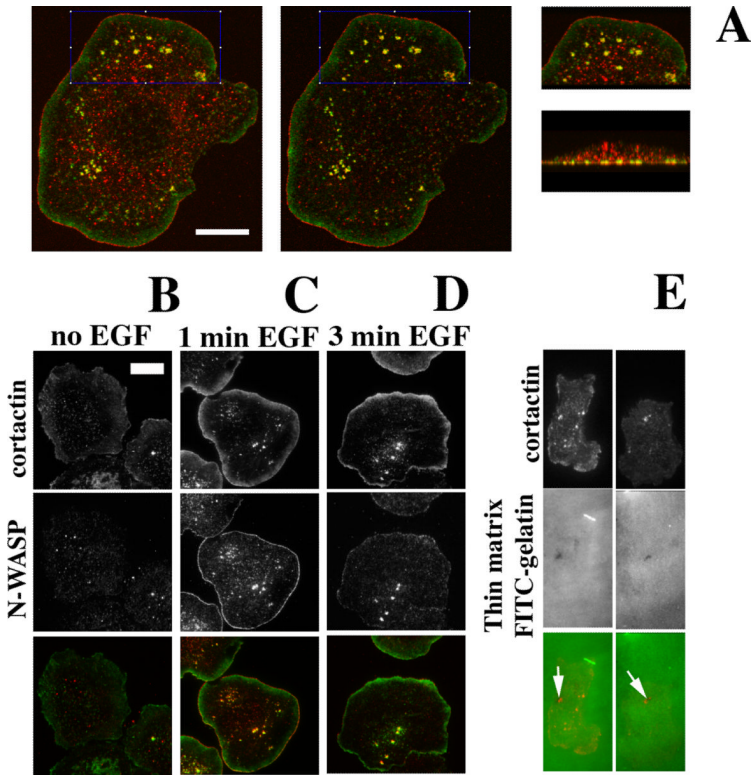


**Figure 1. After EGF stimulation, invadopodia that contain N-WASP and cortactin form at the ventral surface of carcinoma cells on glass**

A. Confocal microscopy: MTLn3 cells were stimulated with EGF for 1 min and labeled for cortactin (green) and N-WASP (red). A. Left panel: Maximum pixel projection through entire z-series. Middle panel: Single optical section at the bottom of the cell. Small panels: Maximum pixel projection through entire z-series, partial boxed image (top) and 90 ° rotation (bottom). Size bar indicates 10 um. B–D. TIRF microscopy: MTLn3 cells were stimulated with EGF for the times indicated and fixed. Cells were stained with antibodies against cortactin (green) and N-WASP (red). Size bar indicates 10 um and applies for B–E. E. Matrix degradation in serum. MTLn3 cells were plated on a thin gelatin matrix labeled with FITC-gelatin (Bowden et al. 2001), followed by fixation and anti-cortactin staining (red). Matrix degradation (dark areas) localizes at cortactin-rich structures at the ventral surface (see arrows).

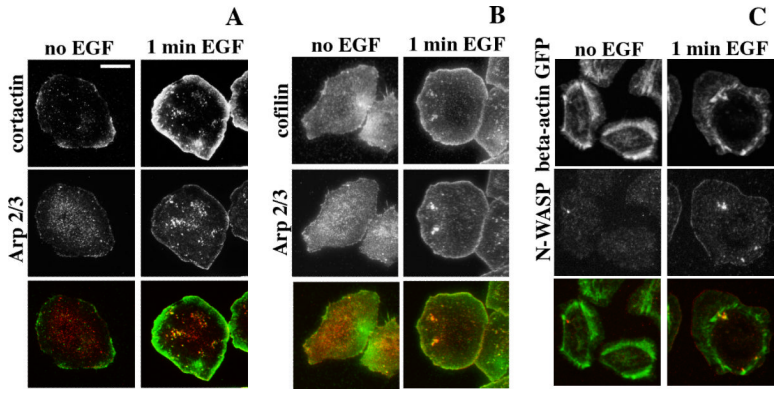


**Figure 2. Invadopodia on glass contain Arp2/3, cofilin and actin**

A. MTLn3 cells were stained with anti-cortactin (green) and anti-Arp2 (red). B. Cells were stained with anti-cofilin (green) and anti-Arp2 (red). C. Cells stably transfected with beta-actin-GFP were stained with anti-N-WASP (red). Bar = 10 um.

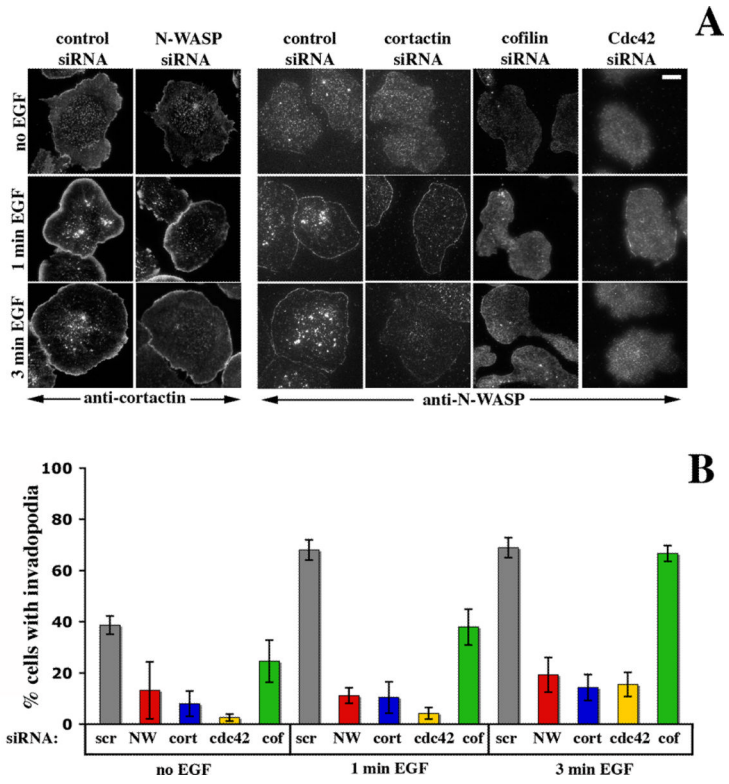


**Figure 3. Depletion of either N-WASP, cortactin or Cdc42 eliminates EGF induced invadopodium formation, while depletion of cofilin slows formation**

MTLn3 cells were treated with siRNA to deplete N-WASP, cortactin, Cdc42, or cofilin or treated with a control siRNA as indicated. A. siRNA treated cells were stimulated with EGF as indicated and stained with antibodies against cortactin (siRNA N-WASP) or N-WASP (siRNA cortactin, siRNA Cdc42 or siRNA cofilin). Cells were imaged by TIRF-microscopy. B. Quantification: Percent of the cells containing invadopodia before and after EGF stimulation. Cells were treated with siRNA as indicated (scr: control siRNA, NW: N-WASP siRNA, cort: cortactin siRNA, cof: cofilin siRNA). Error bars represent SEM, data was derived from at least three separate experiments in each case (for each experiment, 37–56 cells were scored for each condition). Size bar applies to all panels and indicates 10 um.

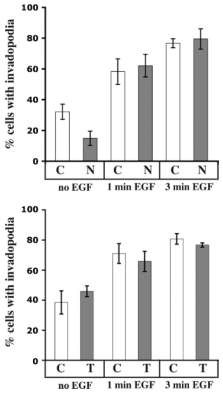


**Figure 4. Disruption or stabilization of microtubules has no effect on the formation of invadopodia after EGF stimulation**

A. Graph: Invadopodium formation after nocodazole treatment. Control cells and cells pretreated with 10 μM nocodazole for 1 hr were stimulated with EGF and stained for invadopodia. B. Graph: Invadopodium formation after taxol treatment. Control cells and cells pretreated with 5 μM taxol for 1 hr were stimulated with EGF and stained for invadopodia.

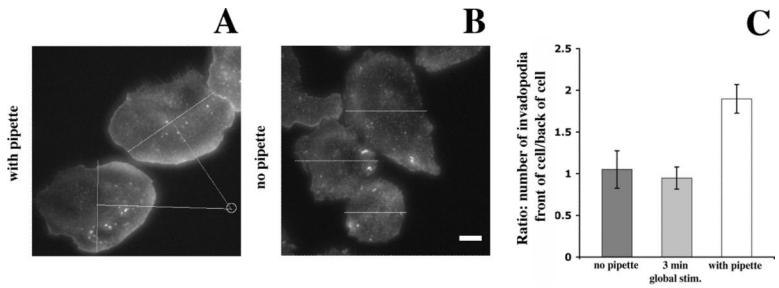


**Figure 5. Invadopodia form preferentially on the side facing an EGF gradient**

A. MTLn3 cells were stimulated with a local EGF gradient using a micropipette for 90 seconds, then fixed after a total of 3 minutes and stained with anti- cortactin (Mouneimne et al. 2004). B. Control cells were not stimulated with EGF and also stained for cortactin. Images were taken by TIRF microscopy. Size bar indicates 10 um. C. Quantification: For pipette-stimulated cells, the location of the pipette-tip is indicated by the circle. A line was drawn from the pipette-tip location to the centroid of the cell. A perpendicular line was then drawn through the centroid of the cell to define front (facing the pipette) and back (facing away from the pipette) of the cell. For control cells, arbitrary horizontal lines were drawn through the centroid of cells. The plot shows the ratio of number of invadopodia in the front versus the back of the cells. Error bars indicate SEM, data was derived from three separate experiments, a total of 40–44 control and 44 EGF stimulated cells were analyzed.

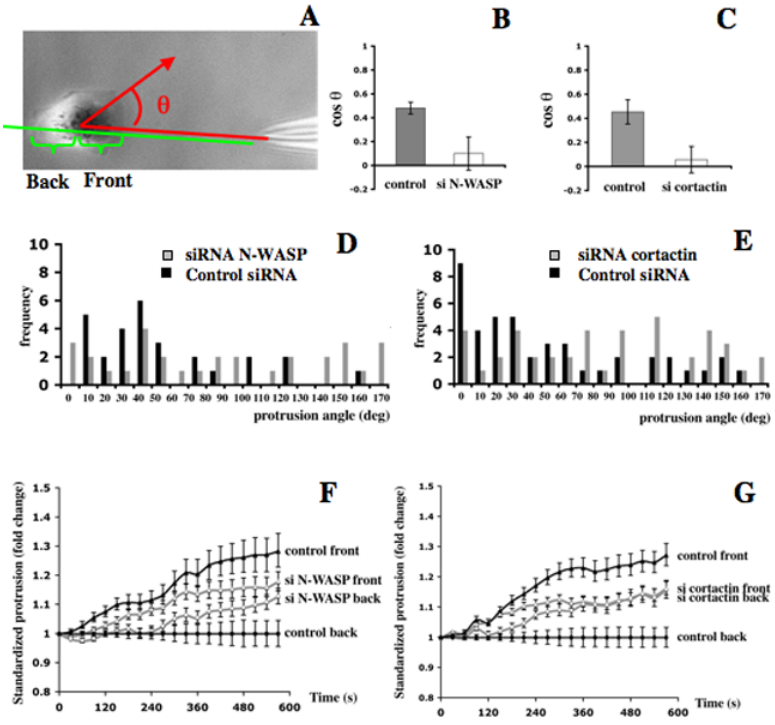


**Figure 6. Cells depleted of N-WASP or cortactin (and thus invadopodia) show a defect in chemotaxis toward a pipette**

MTLn3 cells were starved and then stimulated with EGF for 90 seconds using a micropipette. Time-lapse images were taken during EGF stimulation and for a total of 10 min. A. Phase contrast image of pipette and cells during EGF stimulation. Red lines/arrows indicate chemotactic index (cosθ measurement, where θ is the angle between the line that is drawn between the cell centroid and the pipette tip in the first frame and the line that is drawn between the cell centroid in the first and the last frame of the time-lapse. B. Graph of chemotactic index (cosθ) for cells treated with control or N-WASP siRNA. Error bars are SEM from 27 cells (control) and 35 cells (siRNA N-WASP) pooled from three separate experiments. See supplemental Figure S3 for similar results using dominant negative N-WASP. C. Graph of the chemotactic index (cosθ) for cells treated with control or cortactin siRNA. Error bars are SEM from 43 cells pooled from three separate experiments. D. Angle distribution for control and N-WASP siRNA treated cells. Frequency of angle (number of cells with a particular angle-range) are plotted versus protrusion angle. E. Angle distribution for control and cortactin siRNA treated cells. F,G. Standardized membrane protrusion at the front and back of cells treated with control or N-WASP siRNA (F) or control or cortactin siRNA (G) versus time after micropipette stimulation. Front protrusions were measured as a change in distance between the centroid of the cell and the cell membrane along a line from the centroid of the cell to the pipette tip (see panel A, green markings for a schematic). Back protrusions were measured as a change in distance between the centroid of the cell and the membrane along a line that runs through the pipette tip location and the centroid of the cell and extends to the back membrane (see panel A, green markings for a schematic). All protrusion values were standardized over protrusion values at the back of control cells. The same set of cells was analyzed as for the chemotactic index analysis above. Error bars indicate SEM. Note that the sum of protrusions at the front and back is the same in control and siRNA treated cells.